Published in final edited form as:
Cancer Immunol Res. 2013 November 1; 1(5): . doi:10.1158/2326-6066.CIR-13-0086.

GITR Pathway Activation Abrogates Tumor Immune Suppression Through Loss of Regulatory T cell Lineage Stability

David A. Schaer[1], **Sadna Budhu**[1], **Cailian Liu**[1], **Campbell Bryson**[2], **Nicole Malandro**[1,2], **Adam Cohen**[5], **Hong Zhong**[1], **Xia Yang**[1], **Alan N. Houghton**[1], **Taha Merghoub**[1,*], and **Jedd D. Wolchok**[1,2,4,*]

[1]Swim Across America & Ludwig Collaborative Lab Laboratory, Immunology Program, Sloan-Kettering Institute for Cancer Research, Memorial Sloan-Kettering Cancer Center, New York, NY

[2]Weill Cornell Medical College, Memorial Sloan-Kettering Cancer Center, New York, NY

[4]Ludwig Center for Cancer Immunotherapy at Memorial Sloan-Kettering Cancer Center, New York, NY

[5]Perelman Center for Advanced Medicine, University of Pennsylvania, Philadelphia, PA

Abstract

Ligation of GITR (glucocorticoid-induced tumor necrosis factor (TNF) receptor-related gene, or TNFRSF18) by agonist antibody has recently entered into early phase clinical trials for the treatment of advanced malignancies. Although the ability of GITR modulation to induce tumor regression is well-documented in preclinical studies, the underlying mechanisms of action, particularly its effects on $CD4^+foxp3^+$ regulatory T cells (Treg), have not been fully elucidated. We have previously demonstrated that GITR ligation *in vivo* by agonist antibody DTA-1 causes a >50% reduction of intra-tumor Treg with down modulation of Foxp3 expression. Here we show that the loss of Foxp3 is tumor-dependent. Adoptively-transferred $Foxp3^+$Treg from tumor-bearing animals lose Foxp3 expression in the host when treated with DTA-1, whereas Treg from naïve mice maintain Foxp3 expression. GITR ligation also alters the expression of various transcription factors and cytokines important for Treg function. Complete Foxp3 loss in intra-tumor Treg correlates with a dramatic decrease in Helios expression and is associated with the upregulation of transcription factors T-Bet and Eomes. Changes in Helios correspond with a reduction in IL-10 and an increase in IFNγ expression in DTA-1-treated Treg. Together, these data show that GITR agonist antibody alters Treg lineage stability inducing an inflammatory effector T cell phenotype. The resultant loss of lineage stability causes Treg to lose their intra-tumor immune suppressive function, making the tumor susceptible to killing by tumor-specific effector $CD8^+$ T cells.

Keywords

GITR; Foxp3; Helios; Regulatory T cell Lineage Stability; Intra-tumor Immune suppression

Introduction

The immune system is capable of recognizing malignant cells, but in most situations, tumors develop strategies to avoid elimination and escape immune surveillance [1]. Recent

Corresponding Author: Jedd D. Wolchok, MD, PhD: wolchokj@mskcc.org.
*Co-Senior Authorship

Conflict of Interest Statement: The authors have no conflicts to disclose

advances in immunotherapy have succeeded in shifting the balance from tumor immune escape to tumor elimination. Instead of treating the tumor directly by inhibiting cell growth, immunotherapeutic approaches modulate a patient's immune system to induce tumor regression. The success of this approach is highlighted by the FDA approval of the CTLA-4-blocking antibody ipilimumab, the first therapy to demonstrate enhanced overall survival for patients with melanoma [2]. Serving as a proof of principle, CTLA-4 blockade has led to targeting of other immune checkpoints (PD-1 / PD-L1) alone or in combination with CTLA-4, with very promising results in early phase clinical trials [3–6]. Although co-inhibitory receptor blockade has demonstrated durable clinical efficacy, a significant number of patients (~50–80%) remain refractory to these treatments and some tumor types do not respond as robustly as others [3,7]. To further potentiate antitumor immune responses and extend clinical benefit, activating co-stimulatory molecules, such as TNF receptor superfamily members GITR, OX40, and 4-1BB represents a logical next step [8,9].

GITR became an attractive target for cancer immunotherapy after the agonistic anti-GITR antibody DTA-1 was shown to block the suppressive effects of regulatory T cells (Treg) [10]. Subsequently, DTA-1 was shown to enhance tumor immunity in a concomitant immunity model of melanoma. In addition to preventing growth of secondary tumor challenges, DTA-1 treatment also caused the regression of some of the primary challenge tumors [11]. This observation has been extended into multiple tumor models and various combinatorial strategies with vaccines, adoptive T cell transfer and concurrent CTLA-4 blockade [12]. With preclinical success of GITR tumor immunotherapy, it has been entered into early phase clinical trials for the treatment of advanced malignancies. Despite its therapeutic potential, the mechanism of action on Treg as opposed to effector T cells (Teff) has not been fully elucidated. Understanding its activity on Treg is a necessary step to inform the effective use of GITR therapy in humans.

Whether or not GITR immunotherapy targets GITR solely on Teff, or on both Teff and Treg is under investigation. Because GITR is constitutively expressed at high levels on Treg, it was assumed that DTA-1 directly inhibited Treg suppressive function *in vitro* [10]. However, GITR is also upregulated on CD4 and CD8 Teff following activation and acted as co-stimulatory receptor [13]. Through the use of $GITR^{-/-}$ Treg, it was determined that the co-stimulatory role of GITR enabled Teff to resist Treg suppression while having no direct effect on Treg [14]. Thus, initial reports of enhanced tumor immunity resulting from GITR ligation by agonist antibody DTA-1 was attributed to the modulation of Teff [15,16]. Nevertheless, we and others have recently shown that direct modulation of Treg is an important consequence of DTA-1 therapy [17,18]. DTA-1 treatment causes >50% reduction of intra-tumor Treg and down modulation of Foxp3. In addition, the effects of DTA-1 are attenuated if either Teff or Treg is $GITR^{-/-}$ [17]. Our data suggest that the efficacy of DTA-1 comes not only from its effect on Teff but also from its modulation of Treg.

Here we demonstrate that GITR ligation by DTA-1 induces intra-tumor Treg lineage instability. DTA-1 causes loss of Foxp3 in a tumor-dependent manner and is preceded by the loss of the transcription factor Helios. This results in the acquisition of a Th1 effector-like profile and prevents Treg-mediated intra-tumor suppression of the antitumor immune response. Our results demonstrate that modulation of Treg, along with Teff, is important and necessary for the efficacy of GITR immunotherapy.

Materials and Methods

Mice

C57BL/6: CD45.1, Thy1.2+, Thy1.1+ and OT-1TCR transgenic mice were obtained from Jackson Laboratory (Bar Harbor, ME). Pmel-1 T-cell receptor transgenic mice were a gift

from Dr. Nicohlas Restifo (NCI, MD). Foxp3GFP knock-in mice were a gift from Dr. A. Rudensky (MSKCC, NY, NY) GITR$^{-/-}$ and GITR$^{+/+}$ littermates (Sv129 × C57BL/6 background) were a gift from Dr. P.P. Pandolfi (MSKCC, NY, NY) and were backcrossed >10 generations and onto Pmel-1 Thy1.1+ C57BL/6 background using a speed congenic system. Mice were maintained according to NIH Animal Care guidelines, under a protocol (# 96-04-017) approved by the MSKCC Institutional Animal Care and Use Committee.

Cell lines, tumor challenge and DTA-1 therapy

B16F10/LM3 (hereafter called B16) is derived from the B16F10 line provided by I. Fidler (M.D. Anderson Cancer Center, Houston, TX), and transfected with OVA to generate B16-OVA [19]. Tumor cells were cultured in RPMI 1640 medium containing 7.5% FBS (for up to 2 weeks after thawing). Each mouse received 150,000 cells in 150μl of growth factor-reduced Matrigel (BD Biosciences) injected subcutaneously. Four days after tumor challenge, mice were injected intraperitoneally with either 1 mg of affinity-purified DTA-1 or Purified Rat IgG (Sigma-Aldrich) in 500 μL PBS.

Lymphocyte isolation

Spleens, tumor draining lymph nodes (TDLNs), and tumors were excised on days indicated in the text. Tumors were weighed, and then tissue was homogenized through 40μm strainers to produce single cell suspensions. RBCs were lysed from spleens using an ACK lysis buffer (Lonza). Cells were washed with media, and tissue cell counts were calculated using Guava cell counter (Milipore). Cells were then either: sorted for Treg, stained immediately by FACS, or for cytokine recall: stimulated with PMA and Ionomycin for 4 hours and then treated with monensin before FACS staining.

Antibodies and FACS analysis

Anti-GITR (DTA-1, S. Sakaguchi, Osaka University, Osaka, Japan), and anti-OX40 (OX86, A. Weinberg, Earle Chiles Research Institute, Portland, OR), were produced by the MSKCC Monoclonal Antibody Core Facility, anti-4-1BB (LOB12.3) was procured from Bioxcell. Foxp3 Staining Kit (eBioscience,) was used for intracellular staining. Antibodies to antigens listed in figures were from BD Biosciences except: Foxp3 (eBioscience), Helios, CD45.2 (Biolegend), Nrp1 (R&D systems). Dead cell exclusion was done using the Aqua LIVE/DEAD® Fixable Dead Cell Stain Kit (Invitrogen). Samples were acquired on 12-color LSRII cytometer, and analyzed using FlowJo (Treestar).

Treg Adoptive Transfers

Tumor-experienced or naïve Foxp3-GFP Treg were isolated from spleens and tumor draining lymph nodes (TDLNs) of untreated Foxp3-GFP mice bearing B16 tumors 7–8 days after tumor challenge, or non-tumor-bearing mice. CD4$^+$ GFP$^+$ Treg were isolated by enriching CD4$^+$ cells by CD4 positive or negative MACS microbead separation kits (Miltenyi) before sorting for GFP expression on a Cytomation MoFlo or BD FACS Aria cell sorter in the MSKCC Flow Cytometry Core Facility. For co-transfer experiments (Fig 1C), naïve Treg were isolated from Thy 1.1$^+$ C57BL/6 mice using MACS microbead Treg isolation kit (Miltenyi). Treg were then injected intravenously (5–7×10^{5}cell/mouse for each Treg type being transferred) in 200 μl of sterile PBS.

Collagen-Fibrin gel Killing assay

The collagen-fibrin gel killing assay is described in depth in reference [20] and was adapted for *ex vivo* tumors. Briefly: B16-Ova Tumors isolated on day 10 or 11 after tumor challenge were cut into small pieces, incubated for 5 min in 250μg/ml collagenase in PBS containing $Ca^{2+}Mg^{2+}$ and homogenized through 100μm cell strainers to create single cell suspensions.

Viable tumor cells and tumor infiltrating lymphocytes were counted by trypan blue exclusion. 10^4 viable tumor cells, together with all infiltrating cells were co-embedded into collagen-fibrin gels with or without $1–5\times10^5$ $CD8^+$ T cells activated *in vitro* by cognate peptide + IL-2. Duplicate gels were lysed every 24h for 3 days, and viable remaining tumor cells were diluted and plated in 6-well plates for colony formation. 7 days later, plates were fixed with 3.7% formaldehyde and stained with 2% Methylene blue before counting as described in [20].

Rate of tumor cell killing

Killing constant *k* is calculated as described in [20]. Briefly: *k* is calculated according to the following equation: bt = b0e-kpt+gt, where bt = the concentration of B16 cells at time t; b0 = the concentration of B16 cells at time 0; *k* = the killing rate constant (or killing efficiency) for CD8 T cells; p = the concentration of *in vitro* activated CD8 T cells; g = the growth rate constant for B16 cells.

Quantitative PCR

Individual tumors and pooled control spleens were collected and stained with anti-CD45, anti-CD4 and DAPI before $CD45^+$ $CD4^+$ GFP^+ Treg, or GFP^- Teff control, were FACS sorted on BD FACS Aria directly into Trizol reagent (Invitrogen). Total RNA was prepared and reversed transcribed into cDNA using a High Capacity cDNA Reverse Transcription Kit (Applied Biosystems, Grand Island, NY). The primer-probe sets were from TaqMan Gene Expression Assays (Applied Biosystems). Quantitative real time PCR reactions were prepared with FasStart Universal Probe master (Rox) mix (Roche) according to the manufacturer's instructions and done using the ABI 7500 Real Time PCR system (Applied Biosystems). Each gene was amplified in duplicate and repeated in two separate experiments. cDNA concentration differences were normalized to GAPDH. Relative gene expression of the target genes was calculated by the formula $2 - \Delta Ct$ (ΔCt = Ct (target gene) – Ct (GAPDH)).

Results

Tumor growth sensitizes Treg to DTA-1-induced Foxp3 loss

We previously demonstrated that optimal GITR agonist antibody DTA-1 treatment of early established (Day 4) B16 tumors caused intra-tumor Treg to lose Foxp3 expression. By treating tumors grown in mice where Treg express GFP fused in frame to Foxp3 (Foxp3-GFP), we were able to detect remnant GFP protein in former Treg, after Foxp3 had been degraded (Fig 1A). GFP remains, while Foxp3 is degraded, because it is less susceptible to proteolytic degradation (Fig 1A) [17]. DTA-1-induced Foxp3 loss is not seen in peripheral tissues, suggesting that entry into the tumor microenvironment promotes Treg instability and increases susceptibility to modulation [17]. In addition, adoptively-transferred Treg sorted from spleens and TDLNs of tumor-bearing Foxp3-GFP mice lose Foxp3 expression within 48hours of infiltrating tumors in DTA-1-treated hosts [17]. To determine what renders Treg susceptible to GITR modulation, we utilized the adoptive transfer system to track highly purified previously untreated Treg and probe the specific conditions permitting DTA-1-induced Foxp3 loss.

Treg have been described to contain a minor population that is less stable and characterized by low CD25 expression. This population is susceptible to Foxp3 loss after long-term transfer (4 weeks) into $Rag^{-/-}$ hosts [21]. Similar results have been shown recently that stimulation with Fc-GITR-L can augment Foxp3 loss after $CD4^+$ T cell transfer into a $RAG^{-/-}$ model of inflammatory bowel disease [22]. Therefore, we first asked if during our short-term (48hr) adoptive transfer conditions, DTA-1 exclusively modulates only the minor

CD25 low population (which at most accounts for only ~10% of Treg). Consistent with published reports, there is a slight loss in the percentage of $Foxp3^+$ Treg in control IgG-treated mice 2 days after transfer (~90% pre-transfer to ~77% after transfer, Fig 1B). In contrast, DTA-1 treatment induced a pronounced reduction in $Foxp3^+$ Treg (~90% $Foxp3^+$ pre-transfer to ~10% $Foxp3^+$ after transfer, Fig 1B). This translates to an average of a 6 (+/− 0.58 SEM) fold decrease in the percentage of $Foxp3^+$ transferred Treg in DTA-1-treated hosts compared to controls. These data confirm that DTA-1 has the potential to modulate all Treg and is not restricted to the minor, unstable $CD25^{low}$ Treg fraction.

Having established the effect of DTA-1 on Treg Foxp3 loss in lymphopenic conditions, we next assessed how the presence of the tumor and/or tumor infiltration affects Treg vulnerability to DTA-1. To accomplish this, we co-transferred congenically marked (with CD45 and Thy1) Treg isolated from spleens and TDLNs of tumor-bearing ($CD45.2^+$) or naïve ($Thy1.1^+CD45.2^+$) donors into lymporeplete naïve or tumor-bearing recipients ($CD45.1^+$) following the scheme in Fig 1C. Naïve Thy 1.1 donor Treg transferred into naïve recipients displayed negligible loss of Foxp3 in peripheral tissues 48hrs after transfer (88% $Foxp3^+$, pre-transfer Fig 1C vs. ~86–91% $Foxp3^+$, in IgG Fig 1D). DTA-1 treatment induced a maximum of 17–18% reduction in naïve $Foxp3^+$ Treg under these conditions (Fig 1D, Spleen IgG vs. DTA-1). In contrast, tumor-experienced $CD45.2^+$ Treg transferred into control IgG-treated hosts, displayed a greater loss of Foxp3 expression (94% $Foxp3^+$ pre-transfer Fig 1C vs. ~72% and ~48% $Foxp3^+$ Treg in Spleen and LN, respectively Fig 1D). DTA-1 treatment enhanced Foxp3 loss in tumor-experienced Treg, which was most evident in the LN where there was ~50% reduction in $Foxp3^+$ Treg in DTA-1-treated animals, as compared to animals treated with control IgG (Fig 1D). In tumor-bearing recipients, DTA-1 treatment further potentiated the decrease in Foxp3 expression in tumor-experienced Treg in the spleen (34% vs. 23%, IgG vs. DTA-1, p=0.025 comparing $\%foxp3^{NEG}$ [(Post Foxp3 purity-Post Transfer Foxp3%)/Post Foxp3 purity] in Fig 1D and 1E). Naïve Treg only displayed a significant loss of Foxp3 expression upon entering the tumor (Fig 1E, 27% drop IgG vs. DTA-1 compared to pre-transfer). Taken together, our data strongly suggest that pre-conditioning of Treg in the presence of tumor or in the tumor microenvironment prior to DTA-1 treatment is important to their susceptibility to Foxp3 loss.

Transferred Treg do not display cleaved caspase-3 and equal numbers of transferred Treg are recovered after DTA-1 treatment for both tumor experienced and naïve Treg (Supplemental Fig S1A, B). Foxp3 loss in tumor-experienced Treg sorted by high CD25 expression appeared to be comparable to those sorted by Foxp3-GFP (Supplemental Figure S1C). Moreover, to address the possibility that $Foxp3^{NEG}$ Treg result from DTA-1-induced proliferation of contaminating Teff, we monitored the proliferation of transferred Teff ($CD4^+$ GFP^{NEG}) sorted from Foxp3-GFP tumor-bearing mice. Supplemental figure 1D shows that $CD4^+$ GFP^{NEG} Teff (sorted from Foxp3-GFP tumor-bearing mice) do not proliferate or accumulate after transfer and DTA-1 treatment. In sum, these data indicate that $Foxp3^{NEG}$ Treg come directly from the $Foxp3^+$ Treg, whose frequency is not reduced as a consequence of cell death, depletion, or proliferation of contaminating Teff.

In addition, we found that the DTA-1-induced Foxp3 loss occurs in a dose-dependent manner (Supplemental figure S1E). Interestingly, agonist antibodies to GITR-related TNFR family members 4-1BB and OX40 did not affect the frequency of $Foxp3^+$ Treg (Supplemental figure S1F). Thus, this effect appears to be uniquely associated with GITR stimulation.

Foxp3 loss correlates with a loss of Helios expression

The data above suggest that lymphopenic conditions and the presence of tumor sensitize Treg to the effects of DTA-1. Additionally, the data imply that DTA-1 has the ability to

modulate a large percentage of the Treg population, which remains viable after loss of Foxp3. Therefore, we hypothesized that in the tumor therapy setting, even the intra-tumor Treg that maintain Foxp3 expression after DTA-1 treatment would be affected by GITR stimulation. In fact, we have previously shown that Foxp3 expression in the remaining Treg is significantly lower in DTA-1- vs. control IgG-treated tumors supporting this concept [17]. To better understand the outcome of DTA-1-induced Treg instability, we investigated if there were changes in other markers associated with Treg stability, function and/or ontogeny such as the transcription factor Helios, and expression of the cell surface VEGF co-receptor Neuropilin 1 (Nrp1). Expression of Nrp1 has been reported to distinguish between thymus-derived (tTreg) and peripherally-derived Treg (pTreg) and is important for Treg trafficking to B16 tumors [23–25]. Although the exact role of the Ikaros family transcription factor Helios remains unresolved, it has been described as a marker of Treg activation and identifies the most suppressive population of tumor-infiltrating Treg [26,27]. In control animals, intra-tumor Treg are uniformly Helios^{HIGH} with a majority being Nrp1^{HIGH}, at the peak of B16 immune infiltration compared to peripheral Treg (Spleen, 10–11 days after tumor challenge [28]), suggesting a highly activated tTreg phenotype (Fig 2A) [25,27]. In contrast, DTA-1 treatment causes a clear loss of Helios expression in the remaining Foxp3^{+} intra-tumor Treg (Fig 2A). Nrp1 expression did not appear to be as significantly affected as Helios, which may be related to its role in Treg trafficking [24].

Using changes in Helios expression as a surrogate marker to identify DTA-1-modulated Treg in addition to Foxp3 loss, we expanded our analysis to early phases of Treg tumor infiltration to determine the kinetics of Helios loss and its possible correlation with Treg survival and function. At day 7 of tumor growth (3 days after DTA-1 treatment), there is already a significant increase in the Helios^{LOW} Treg cell population (~18% compared to ~55% in IgG vs DTA-1 treatment, respectively, Fig 2B, left panel). By day 10, there is a ~55–60% loss of Foxp3^{+} Treg (Supplemental Figure 2A), and the remaining Foxp3^{+} Treg, (~45–50%) are Helios^{LOW} in DTA-1-treated tumors. Taken together these data suggest that ~75–80% of the Treg (compared to control IgG) in the tumor have been modulated by DTA-1.

Helios^{LOW} Treg in DTA-1-treated tumors express more of the pro-survival genes BCL-2 and BCL$_{XL}$ than Helios^{HIGH} or Total IgG Treg (Fig 2B). This phenotype extends to the peak of immune infiltration at day 10, but by day 14, even though the tumors are regressing, the majority of the remaining Treg are Helios^{HIGH} (Fig 2B). Treg with the lowest levels of Helios at day 7, also displayed a pronounced reduction Foxp3 and CD25 (Fig 2C). Helios loss appears to parallel the extent to which free cell surface GITR is saturated/modulated by DTA-1, preventing further staining on Treg (Fig 2D). At day 14, the 1mg/mouse dose of DTA-1 no longer saturates available GITR, and intra-tumor Treg in DTA-1-treated mice display similar Helios expression compared to IgG (Day 14 post tumor challenge in Fig 2B & D). This supports the conclusion that Treg lose Foxp3 expression after tumor infiltration, with gross changes in Helios expression being a reliable marker of GITR modulation. Increased expression of BCL-2 and BCL$_{XL}$, combined with the lack of activated caspase-3 (Supplemental figure 1), shows that modulated Treg maintain a pro-survival phenotype

GITR stimulation alters Treg Lineage stability

Treg naturally co-opt and express inflammatory T cell lineage transcription factors (T-bet, RORγt) to facilitate the suppression of the corresponding Teff program [29,30]. When Foxp3 expression is ablated in Treg, they have been shown to revert to cells with a Teff phenotype. In addition, Helios has been shown to stabilize Treg programming and suppress IL-2 expression [31,32]. Therefore, DTA-1-treated Treg that have lost or are losing Foxp3 expression could acquire a Teff-like phenotype. In contrast to the reduced expression of Foxp3 and CD25 in DTA-1-treated mice, Helios^{LOW} Treg showed increased protein

expression of T cell lineage transcription factors such as T-bet, RORγt and Eomes, compared to Helios^{HIGH} Treg (Fig 3A). Expression in Helios^{LOW} Treg was also higher than Treg in the IgG control groups at multiple time points (Day 7 for T-bet, D7–14 for Eomes, D10 and 14 for RORγt, Fig 3A).

To determine if increased T-bet, RORγt and Eomes protein levels in Treg has biological consequence, we performed a cytokine recall assay on cells isolated from tumors 10 days after DTA-1 treatment. Foxp3-GFP mice were used for this experiment since the staining for Foxp3 and Helios is diminished and unreliable after PMA/Ionomycin stimulation (Supplemental figure S2B). Using Foxp3-GFP mice also allowed us to circumvent this technical hurdle as low levels of Foxp3 expression correlates with loss of Helios (Fig 2C), allowing us to subset our analysis to Foxp3-GFP^{LOW} and Foxp3-GFP^{HIGH} Treg. GFP^{LOW} Treg (Helios^{LOW}) in DTA-1-treated mice showed a >2 fold increase in IFN-γ production compared to control IgG-treated Treg (Fig 3B). While there was no difference in the IFN-γ expression between GFP-high and -low cells in IgG control tumors (Fig 3B top), IFN-γ expression was restricted to GFP^{LOW} in DTA-1-treated Treg (Fig 3B bottom). Despite increased RORγt expression in Helios^{LOW} Treg, we did not detect any significant difference between IgG and DTA-1-treated Treg in its related cytokine IL-17 (data not shown). In order to confirm this result and more closely measure changes in Treg lineage phenotype, we sorted Foxp3-GFP Treg from individual tumors and measured the expression of relevant Treg and Teff genes. Using this approach, we found a maximum of 4-fold upregulation in IFN-γ expression (Day 7) and ~2-fold decrease in IL-10 expression (Day 10) in DTA-1-treated Treg (Fig 3C). Other markers, such as GITR, IL-2, IL-17, TNFα, TGFβ and SATB1 were expressed to equivalent levels in DTA-1-treated and IgG-treated Treg (data not shown). Although Helios protein levels after DTA-1 treatment correlated with reduced Helios gene expression, there was no major difference in Foxp3 gene expression (Fig 3D). This would indicate that GITR signaling may cause a post transcription modification that leads to reduced Foxp3 protein expression. Regardless of the mechanism responsible for the loss of Foxp3 and Helios expression, these results suggest that DTA-1 induces Treg lineage instability and acquisition of a Teff-like profile.

DTA-1-induced lineage instability removes Treg suppressive function from the tumor

In order to determine if the phenotypic changes described above alter Treg suppressive function *in vivo*, we utilized an *ex-vivo* collagen-fibrin gel matrix culture to measure CD8$^+$ T cell cytolytic (CTL) effector function against tumor cells from control IgG- or DTA-1-treated mice [20]. Collagen-fibrin gels mimic a three-dimensional tissue-like environment and are more sensitive than packed-cell-pellet assays at measuring CD8$^+$ CTL effector function [20]. Furthermore, we have found that collagen-fibrin gel cultures of explanted B16 or B16 expressing OVA (B16-OVA) tumors, which include all infiltrating cells, are resistant to killing by a 10–50 fold excess of *in vitro* cognate antigen activated CD8$^+$ CTL, recapitulating the suppression that exists *in vivo* (Fig 4A and Budhu & Schaer, unpublished).

Consistent with prior results, control IgG-treated tumors become resistant to killing by *in vitro* activated CTLs and proliferate in the collagen gels after 24 hours, with the number of tumor cells increasing overtime (Fig 4A and Budhu & Schaer, unpublished). In contrast, DTA-1 treatment caused tumors to remain susceptible to *ex vivo* killing by activated CTLs, and the number of viable tumor cells continues to decrease at 48 and 72hrs (2 fold & 3 fold, respectively, vs. 0hr, Fig 4A). Calculation of the killing efficiency, *k* (as described in methods and in ref [20]) highlights the differences between DTA-1- and control IgG-treated tumors. Killing efficiency of CTLs in DTA-1-treated tumors increases over 2 fold at 48 hrs (5.3×10^{-10} at 24hrs to 1.3×10^{-9} at 48hrs, Fig 4A) in contrast to that in IgG-treated mice, which maintains suppression. *Ex vivo* addition of DTA-1 had no effect on the killing of

DTA-1-treated tumors, control IgG-treated tumors or cultured B16 cells, and GITR $^{-/-}$ CTL kill tumor cells from DTA-1-treated tumors and cultured B16 cells at the same rate as GITR$^{+/+}$ CTL (Fig 4B, dashed lines and green lines vs red lines). This suggests that killing is independent of GITR stimulation by DTA-1 on CTL (Fig 4B). Combined, our data support the conclusion that GITR modulation of Treg by DTA-1 removes their suppressive influence in the tumor microenvironment.

Discussion

The overarching goal of cancer immunotherapy has been the activation of tumor-specific immunity that is able to overcome the hurdles established by tumors to evade immune destruction. GITR activation appears to reach an important balance by enhancing tumor immunity while inhibiting immune suppression in a tumor-dependent manner. The research presented here shows that in addition to its established role in modulating Teff, DTA-1 treatment causes Treg to lose lineage stability, reducing their suppressive influence over the tumor microenvironment.

Our data suggest that conditions present in tumor-bearing mice and the tumor microenvironment are responsible for making Treg susceptible to GITR-induced Foxp3 loss. Reduced IL-2 levels have been shown to be important for Treg stability and homeostasis [33,34]. However, we do not believe the lack of IL-2 accounts for Treg instability in our system, since transferred Treg lose Foxp3 in the periphery even after transfer into lymphoreplete hosts. In addition, equal numbers of co-transferred tumor-experienced and naïve Treg are recovered from DTA-1-treated animals, despite the loss of Foxp3 expression in tumor-experienced Treg. This suggests that DTA-1 does not simply deplete Foxp3^{+} Treg (Supplemental figure S1B, Fig 1D). Only upon tumor infiltration in DTA-1-treated animals do naive donor Treg manifest significant Foxp3 loss, highlighting further the role of tumor conditioning on Treg and even at steady state. Therefore, while the detailed mechanism of GITR signaling-induced Foxp3 loss requires further investigation, it is evident that tumor-preconditioning and the tumor microenvironment play a major role in permitting GITR-dependent modulation of Foxp3 expression.

The reduction of CD25 expression and the production of IFN-γ observed in intra-tumor Treg during DTA-1 therapy (Fig 2,3) are similar to what has been reported when Foxp3 is deleted in mature Treg [35]. There has been evidence suggesting that inflammatory environments cause Treg to lose stability and convert to a Teff-like phenotype [29]; however recent research has brought these findings into question. Results from Hori's group suggest that the conversion of Treg into Teff is actually due to a transient expression of Foxp3 in non-Treg [36,37]. It is unlikely that the DTA-1-induced Treg lineage conversion we observe here is an artifact of lineage marking. The Treg-transfer and gene expression analysis experiments (Fig 1, 3) rely on sorting an entire Foxp3-GFP positive Treg population and do not use a lineage-marking Cre recombinase system. In fact, we were unable to use Foxp3-Cre mice due to the "leaky" lineage-marking seen during backcrossing to the C57BL/6 background (data not shown). Thus, we believe the results presented here illustrate that DTA-1-mediated GITR stimulation causes tumor-specific reprogramming of Treg into a Teff-like phenotype. As we were unable to isolate or phenotype repolarized Foxp3^{-} Treg using the Foxp3-Cre lineage-marking mice, it remains to be established if the conversion of Treg to a Teff-like profile is necessary or secondary to the loss of Foxp3/suppressive function. Development of complex genetic models would be needed to answer this question and determine if former DTA-1-modulated Treg work to potentiate antitumor immunity after losing suppressive capacity.

How DTA-1-induced GITR signaling leads to Foxp3 degradation is an important question. Expression levels of Foxp3 mRNA were comparable between control IgG- and DTA-1-

treated mice, but there is a marked reduction in Foxp3 protein levels (Fig 3B, 2C). This would suggest that downstream signaling from GITR imposes post-transcriptional or post-translational control of Foxp3 protein expression. While downstream signaling from GITR induced by GITR-L was recently shown to alter Treg suppressive function through the activation of JNK, it is unclear whether DTA-1 causes a similar effect [38]. JNK activation after long-term GITR-L stimulus resulted in reduced Foxp3 mRNA expression to a level which we did not observe with DTA-1 treatment. GITR and TNFR family members utilize TNFR-associated Factor (TRAF) proteins to transmit downstream signals [8,39]. As many TRAF proteins function as E3 ubiquitin ligases, one hypothesis could be that overstimulation of GITR by DTA-1 could cause an intersection of this cascade with Foxp3 protein and targeting it for degradation. Since intra-tumor Treg express less Foxp3 mRNA than peripheral Treg (Fig 3B), this may make them uniquely sensitive to GITR-induced degradation of Foxp3.

A propensity to modulate pTreg over tTreg would be a logical assumption considering their unstable nature [29]. However, in the case of B16 melanoma, it appears that the majority of intra-tumor Treg have a tTreg-like phenotype as has been seen in 4T1 tumors, and without a minor pTreg population as seen in other tumors [25]. In fact, transfer experiments into $Rag^{-/-}$ mice established that a majority of Treg can be rendered susceptible to GITR-induced loss of Foxp3. We found a similar result, with 75–80% of Treg modulated in the tumor microenvironment during DTA-1 therapy in WT mice (% of intra-tumor Treg Foxp3 loss + % $Foxp3^{+}Helios^{LOW}$ Treg, Supplemental figure S2A, S2B). This suggests that the effects of DTA-1 are not limited to a minor subset of Treg, such as pTreg. Regardless, DTA-1 treatment caused Treg to lose Helios protein and gene expression, corresponding with increased levels of inflammatory T cell transcription factors T-bet, RORγt and Eomes. Treg expression of T-bet or RORγt is not unprecedented and the expression of these transcription factors is important for the Treg suppressive function [29]. Surprisingly Eomes, traditionally thought of as a $CD8^{+}$ CTL transcription factor, is highly upregulated in the DTA-1-treated Treg. We have reported recently that simulation of the closely related TNFR family member OX40 has the ability to induce Eomes in CD4 Teff [40]. Even though there has been evidence that Treg could control immunity through granzyme-dependent killing of B cells, to date no role for Eomes in Treg function has been described [41]. The significance of Eomes expression in DTA-1 modulation of Treg will require further investigation, however, it exemplifies the level to which overstimulation of GITR on susceptible Treg can alter their lineage program

The end result of Treg lineage instability caused by GITR immunotherapy is the removal of intra-tumor suppression mediated by Treg, as demonstrated by the collagen-fibrin gel killing assay (Fig 4). Using the same approach, we recently determined that intra-tumor immune suppression in B16 tumors is Treg-dependent, as specific *in vivo* depletion of Treg restores killing of explanted tumors (Budhu & Schaer, unpublished). Whether or not the DTA-1 effect is due to reduced intra-tumor Treg numbers, Treg lineage instability or a combination of both remains to be determined. Interestingly, even though GITR treatment removes Treg suppression and DTA-1-treated tumor are regressing *in* vivo, tumor cells co-culture with total infiltrates continue to grow e*x vivo* (Fig 4). We interpret the need for additional input of effector T cells to continue killing as evidence that for optimal *in vivo* therapy, GITR's ability to enhance $CD8^{+}$ T cell numbers and persistence also plays an important role [42]. Consequently, targeting Treg appears to be a major mechanism for DTA-1 treatment along with its intrinsic effects on $CD8^{+}$ T cells. This conclusion is in agreement with our prior results demonstrating that both Treg and Teff must express GITR for the optimal effects of DTA-1 [17].

Development of new immunotherapies that accelerate antitumor immunity is important, as checkpoint blockade does not benefit all patients [2,3]. Our data shows that ligation of GITR can accomplish both goals. By inducing Treg lineage instability, DTA-1 releases an important source of suppression of tumor immunity. At the same time, we and others have demonstrated that GITR ligation by DTA-1 accelerates antitumor immunity to take advantage of the now permissive tumor microenvironment [12,17]. The unique ability of GITR ligation to target both axes, modulating Treg primarily in the tumor microenvironment, supports the continued clinical development of GITR agonist agents. Accordingly, in collaborations with GITR Inc., we are currently investigating the agonist anti-human GITR antibody TRX-518 in a phase 1 first in human trial (GITR Inc., Clinical trials.gov: NCT01239134). We believe that the knowledge gained from our study in understanding GITR mechanism of action will help facilitate the development of appropriate biomarkers and inform rational design of future clinical trials.

Supplementary Material

Refer to Web version on PubMed Central for supplementary material.

Acknowledgments

The Authors would like to thank current and former Wolchok Lab members; Dr. Stephanie Terzulli, Andre Burey, Judith Murphy, Kelly Crowley, Rodger Pellegrini, Dr. Arvin Yang, and Dr. Francesca Avogadri for their support on the GITR project. Rudensky lab members; Dr. Steve Josefowicz, Dr. Rachel Niec, Dr. Ashutosh Chaudhry, and Dr. Robert Samstein for generous sharing of reagents and always being available for advice and thoughtful discussion regarding Treg lineage stability. Dr. Joe Ponte for valuable shared insight on the mechanism of GITR immunotherapy. Dr. Michael Curran for assistance with experimental design. Members of the MSKCC flow cytometry, and molecular cytology core facilities. Dr. Roberta Zappasodi for her very helpful comments, critical reading and editing of this manuscript.

Funding

This study was supported by NIH grants R01CA56821, P01CA33049, and P01CA59350 (to J.D.W. and A.N.H.), D.A.S was supported by the NIH Clinical Training for Scholar Grant K12 CA120121-01, and received support from the NIH/NCI Immunology Training Grant T32 CA09149-30 and John D. Proctor Foundation: Margaret A. Cunningham Immune Mechanisms in Cancer Research Fellowship Award; Swim Across America; the Mr. William H. Goodwin and Mrs. Alice Goodwin and the Commonwealth Cancer Foundation for Research and the Experimental Therapeutics Center of Memorial Sloan-Kettering Cancer Center (to J.D.W.)

References

1. Schreiber RD, Old LJ, Smyth MJ. Cancer Immunoediting: Integrating Immunity's Roles in Cancer Suppression and Promotion. Science. 2011; 331:1565–1570. [PubMed: 21436444]
2. Hodi FS, O'Day SJ, McDermott DF, Weber RW, Sosman JA, et al. Improved Survival with Ipilimumab in Patients with Metastatic Melanoma. New England Journal of Medicine. 2010; 363:711–723. [PubMed: 20525992]
3. Topalian SL, Hodi FS, Brahmer JR, Gettinger SN, Smith DC, et al. Safety, activity, and immune correlates of anti-PD-1 antibody in cancer. N Engl J Med. 2012; 366:2443–2454. [PubMed: 22658127]
4. Brahmer JR, Tykodi SS, Chow LQ, Hwu WJ, Topalian SL, et al. Safety and activity of anti-PD-L1 antibody in patients with advanced cancer. N Engl J Med. 2012; 366:2455–2465. [PubMed: 22658128]
5. Hamid O, Robert C, Daud A, Hodi FS, Hwu W-J, et al. Safety and Tumor Responses with Lambrolizumab (Anti–PD-1) in Melanoma. New England Journal of Medicine.
6. Wolchok JD, Kluger H, Callahan MK, Postow MA, Rizvi NA, et al. Nivolumab plus Ipilimumab in Advanced Melanoma. New England Journal of Medicine.

7. Royal RE, Levy C, Turner K, Mathur A, Hughes M, et al. Phase 2 trial of single agent Ipilimumab (anti-CTLA-4) for locally advanced or metastatic pancreatic adenocarcinoma. J Immunother. 2010; 33:828–833. [PubMed: 20842054]
8. Snell LM, Lin GHY, McPherson AJ, Moraes TJ, Watts TH. T-cell intrinsic effects of GITR and 4-1BB during viral infection and cancer immunotherapy. Immunological Reviews. 2011; 244:197–217. [PubMed: 22017440]
9. Weinberg AD, Morris NP, Kovacsovics-Bankowski M, Urba WJ, Curti BD. Science gone translational: the OX40 agonist story. Immunological Reviews. 2011; 244:218–231. [PubMed: 22017441]
10. Shimizu J, Yamazaki S, Takahashi T, Ishida Y, Sakaguchi S. Stimulation of CD25(+)CD4(+) regulatory T cells through GITR breaks immunological self-tolerance. Nat Immunol. 2002; 3:135–142. [PubMed: 11812990]
11. Turk MJ, Guevara-Patino JA, Rizzuto GA, Engelhorn ME, Sakaguchi S, et al. Concomitant tumor immunity to a poorly immunogenic melanoma is prevented by regulatory T cells. J Exp Med. 2004; 200:771–782. [PubMed: 15381730]
12. Schaer DA, Murphy JT, Wolchok JD. Modulation of GITR for cancer immunotherapy. Curr Opin Immunol. 2012; 24:217–224. [PubMed: 22245556]
13. Kanamaru F, Youngnak P, Hashiguchi M, Nishioka T, Takahashi T, et al. Costimulation via Glucocorticoid-Induced TNF Receptor in Both Conventional and CD25+ Regulatory CD4+ T Cells. The Journal of Immunology. 2004; 172:7306–7314. [PubMed: 15187106]
14. Stephens GL, McHugh RS, Whitters MJ, Young DA, Luxenberg D, et al. Engagement of glucocorticoid-induced TNFR family-related receptor on effector T cells by its ligand mediates resistance to suppression by CD4+CD25+ T cells. J Immunol. 2004; 173:5008–5020. [PubMed: 15470044]
15. Ramirez-Montagut T, Chow A, Hirschhorn-Cymerman D, Terwey TH, Kochman AA, et al. Glucocorticoid-Induced TNF Receptor Family Related Gene Activation Overcomes Tolerance/Ignorance to Melanoma Differentiation Antigens and Enhances Antitumor Immunity. J Immunol. 2006; 176:6434–6442. [PubMed: 16709800]
16. Cohen AD, Diab A, Perales MA, Wolchok JD, Rizzuto G, et al. Agonist anti-GITR antibody enhances vaccine-induced CD8(+) T-cell responses and tumor immunity. Cancer Res. 2006; 66:4904–4912. [PubMed: 16651447]
17. Cohen AD, Schaer DA, Liu C, Li Y, Hirschhorn-Cymmerman D, et al. Agonist Anti-GITR Monoclonal Antibody Induces Melanoma Tumor Immunity in Mice by Altering Regulatory T Cell Stability and Intra-Tumor Accumulation. PLoS One. 2010; 5:e10436. [PubMed: 20454651]
18. Coe D, Begom S, Addey C, White M, Dyson J, et al. Depletion of regulatory T cells by anti-GITR mAb as a novel mechanism for cancer immunotherapy. Cancer Immunology, Immunotherapy. 2010; 59:1367–1377. [PubMed: 20480365]
19. Wang S, Bartido S, Yang G, Qin J, Moroi Y, et al. A Role for a Melanosome Transport Signal in Accessing the MHC Class II Presentation Pathway and in Eliciting CD4+ T Cell Responses. The Journal of Immunology. 1999; 163:5820–5826. [PubMed: 10570265]
20. Budhu S, Loike JD, Pandolfi A, Han S, Catalano G, et al. CD8+ T cell concentration determines their efficiency in killing cognate antigen-expressing syngeneic mammalian cells in vitro and in mouse tissues. Journal of Experimental Medicine. 2010; 207:223–235. [PubMed: 20065066]
21. Komatsu N, Mariotti-Ferrandiz ME, Wang Y, Malissen B, Waldmann H, et al. Heterogeneity of natural Foxp3+ T cells: A committed regulatory T-cell lineage and an uncommitted minor population retaining plasticity. Proceedings of the National Academy of Sciences. 2009; 106:1903–1908.
22. Ephrem A, Epstein AL, Stephens GL, Thornton AM, Glass D, et al. Modulation of Treg cells/Teffector function by GITR signaling is context-dependent. Eur J Immunol. 2013
23. Yadav M, Louvet C, Davini D, Gardner JM, Martinez-Llordella M, et al. Neuropilin-1 distinguishes natural and inducible regulatory T cells among regulatory T cell subsets in vivo. The Journal of Experimental Medicine. 2012; 209:1713–1722. [PubMed: 22966003]

24. Hansen W, Hutzler M, Abel S, Alter C, Stockmann C, et al. Neuropilin 1 deficiency on CD4+Foxp3+ regulatory T cells impairs mouse melanoma growth. The Journal of Experimental Medicine. 2012; 209:2001–2016. [PubMed: 23045606]
25. Weiss JM, Bilate AM, Gobert M, Ding Y, Curotto de Lafaille MA, et al. Neuropilin 1 is expressed on thymus-derived natural regulatory T cells, but not mucosa-generated induced Foxp3+ T reg cells. The Journal of Experimental Medicine. 2012; 209:1723–1742. [PubMed: 22966001]
26. Gottschalk RA, Corse E, Allison JP. Expression of Helios in Peripherally Induced Foxp3+ Regulatory T Cells. The Journal of Immunology. 2012; 188:976–980. [PubMed: 22198953]
27. Zabransky DJ, Nirschl CJ, Durham NM, Park BV, Ceccato CM, et al. Phenotypic and functional properties of Helios+ regulatory T cells. PLoS One. 2012; 7:e34547. [PubMed: 22479644]
28. Schaer DA, Li Y, Merghoub T, Rizzuto GA, Shemesh A, et al. Detection of intra-tumor self antigen recognition during melanoma tumor progression in mice using advanced multimode confocal/two photon microscope. PLoS One. 2011; 6:e21214. [PubMed: 21731676]
29. Hori S. Stability of regulatory T-cell lineage. Adv Immunol. 2011; 112:1–24. [PubMed: 22118405]
30. Chaudhry A, Samstein RM, Treuting P, Liang Y, Pils MC, et al. Interleukin-10 signaling in regulatory T cells is required for suppression of Th17 cell-mediated inflammation. Immunity. 2011; 34:566–578. [PubMed: 21511185]
31. Getnet D, Grosso JF, Goldberg MV, Harris TJ, Yen H-R, et al. A role for the transcription factor Helios in human CD4+CD25+ regulatory T cells. Molecular Immunology. 2010; 47:1595–1600. [PubMed: 20226531]
32. Baine I, Basu S, Ames R, Sellers RS, Macian F. Helios induces epigenetic silencing of il2 gene expression in regulatory T cells. J Immunol. 2013; 190:1008–1016. [PubMed: 23275607]
33. Setoguchi R, Hori S, Takahashi T, Sakaguchi S. Homeostatic maintenance of natural Foxp3+ CD25+ CD4+ regulatory T cells by interleukin (IL)-2 and induction of autoimmune disease by IL-2 neutralization. The Journal of Experimental Medicine. 2005; 201:723–735. [PubMed: 15753206]
34. Fontenot JD, Rasmussen JP, Gavin MA, Rudensky AY. A function for interleukin 2 in Foxp3-expressing regulatory T cells. Nat Immunol. 2005; 6:1142–1151. [PubMed: 16227984]
35. Williams LM, Rudensky AY. Maintenance of the Foxp3-dependent developmental program in mature regulatory T cells requires continued expression of Foxp3. Nat Immunol. 2007; 8:277–284. [PubMed: 17220892]
36. Miyao T, Floess S, Setoguchi R, Luche H, Fehling HJ, et al. Plasticity of Foxp3(+) T cells reflects promiscuous Foxp3 expression in conventional T cells but not reprogramming of regulatory T cells. Immunity. 2012; 36:262–275. [PubMed: 22326580]
37. Zhou X, Bailey-Bucktrout SL, Jeker LT, Penaranda C, Martinez-Llordella M, et al. Instability of the transcription factor Foxp3 leads to the generation of pathogenic memory T cells in vivo. Nature Immunology. 2009; 10:1000–1007. [PubMed: 19633673]
38. Joetham A, Ohnishi H, Okamoto M, Takeda K, Schedel M, et al. Loss of T Regulatory Cell Suppression following Signaling through Glucocorticoid-induced Tumor Necrosis Receptor (GITR) Is Dependent on c-Jun N-terminal Kinase Activation. Journal of Biological Chemistry. 2012; 287:17100–17108. [PubMed: 22461627]
39. Hacker H, Tseng PH, Karin M. Expanding TRAF function: TRAF3 as a tri-faced immune regulator. Nat Rev Immunol. 2011; 11:457–468. [PubMed: 21660053]
40. Hirschhorn-Cymerman D, Budhu S, Kitano S, Liu C, Zhao F, et al. Induction of tumoricidal function in CD4+ T cells is associated with concomitant memory and terminally differentiated phenotype. Journal of Experimental Medicine. 2012; 209:2113–2126. [PubMed: 23008334]
41. Zhao D-M, Thornton AM, DiPaolo RJ, Shevach EM. Activated CD4+CD25+ T cells selectively kill B lymphocytes. Blood. 2006; 107:3925–3932. [PubMed: 16418326]
42. Snell LM, McPherson AJ, Lin GHY, Sakaguchi S, Pandolfi PP, et al. CD8 T Cell-Intrinsic GITR Is Required for T Cell Clonal Expansion and Mouse Survival following Severe Influenza Infection. The Journal of Immunology. 2010; 185:7223–7234. [PubMed: 21076066]

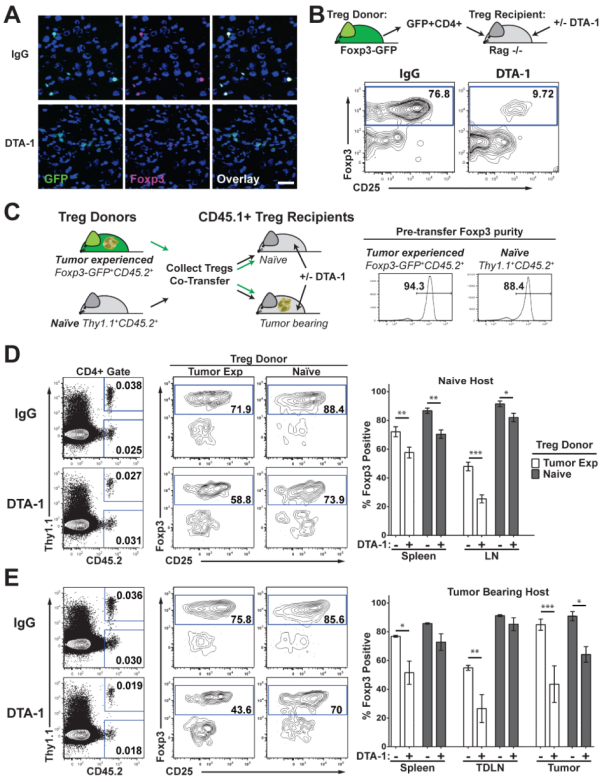

FIGURE 1. Foxp3 loss induced by DTA-1 is enhanced by tumor growth and is increased in the tumor micro environment

A) Fresh frozen sections of B16 tumors from control IgG (IgG)- or DTA-1-treated Foxp3-GFP mice at Day 10 of tumor growth, labeled for Foxp3 and DAPI described in [17]. Scale bar = 25μm. Lack of Foxp3 staining and non-nuclear GFP label is seen in DTA-1-treated sections. **B)** Representative FACS plots show $CD4^+$ transferred Treg in spleen of recipients after gating on Live, $CD45^+$ $CD3^+$, MHC-II^{NEG}, $CD11b^{NEG}$ cells. **C)**Treg were isolated from 25 Naïve Thy1.1 CD45.2 donors and 25 tumor bearing Foxp3-GFP CD45.2 donors, mixed 1:1 and transferred into naïve **(D)**, or tumor-bearing **(E)** CD45.1 recipients treated with IgG or DTA-1. Transferred Treg were identified by gating on live, $CD45^+$, $CD3^+$, $CD4^+$ cells, and then on $CD45.2^+$ (tumor-experienced Treg), or $CD45.2^+$ $Thy1.1^+$ (naïve Treg) (D,E left panels). Representative examples of Foxp3 and CD25 staining is shown in the spleen (D, E middle panels). Graphs show mean +/− SEM for percent of $Foxp3^+$ donor Treg recovered in each tissue from a representative experiment (D, E left panels). Experiments were repeated 3 times with 4–5 per group. * = $p<0.01$, **= $p<0.001$, ***=$p<0.0001$.

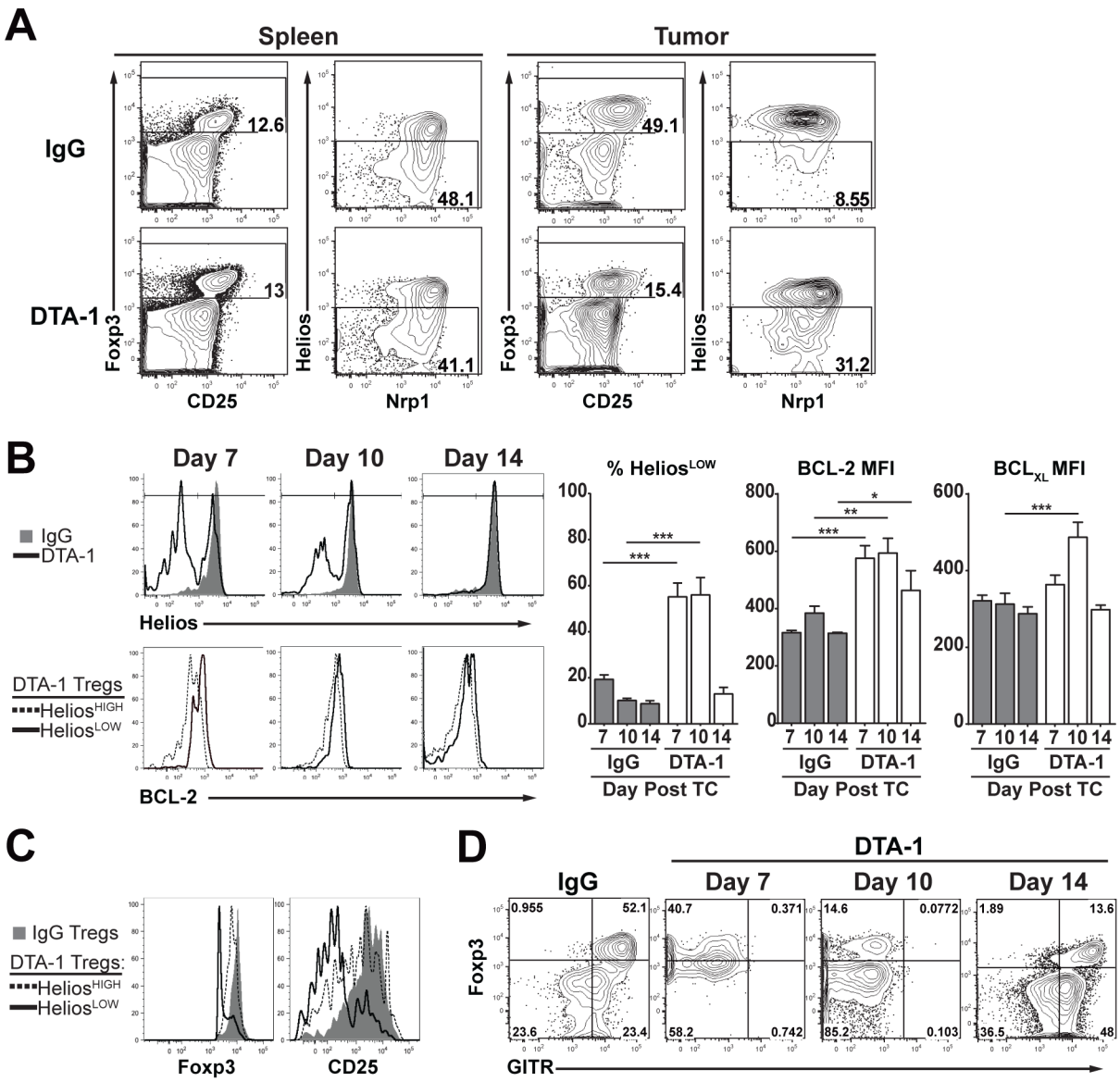

FIGURE 2. DTA-1-modulated Treg show reduced Helios expression and a pro-survival phenotype

A) Representative FACS plots show the percentage of Helios^{LOW} Treg (live, CD45^{+}, CD3^{+}, CD4^{+} Foxp3^{+}) in pooled Spleens and individual Tumors of DTA-1- and IgG-treated mice 11 days after tumor challenge. **B)** Example FACS histograms (top) show Helios expression of IgG- (gray filled) and DTA-1-treated (black line) tumor-infiltrating Treg on indicated day after tumor challenge. Bottom histograms show comparison of BCL-2 expression in Helios^{HIGH} (dashed line) and Helios^{LOW} (solid black line) DTA-1-treated Treg. Mean +/− SEM for the percentage of Helios^{LOW} Treg in IgG- and DTA-1-treated tumors, mean fluorescence intensity (MFI) of BCL-2 and BCL$_{XL}$ for IgG Treg, compared to Helios^{LOW} DTA-1 Treg at each timepoint is shown in the graphs. **C)** Representative Foxp3 and CD25 expression of IgG Treg (gray filed) vs. DTA-1-treated Helios^{HIGH} (dashed line) and Helios^{LOW} (black solid line) Treg, 7 days after tumor challenge. **D)** Example FACS plots show Foxp3 and GITR (DTA-1-PE-Cy7) staining of CD4 T cells in IgG tumors (Day 10 post tumor challenge) compared to DTA-1-treated tumors on day 7, 10 and 14 post tumor

challenge. Experiments were repeated 3 times with 4–5 per group, with one representative experiment shown. * = $p<0.01$, **= $p<0.001$, ***=$p<0.0001$.

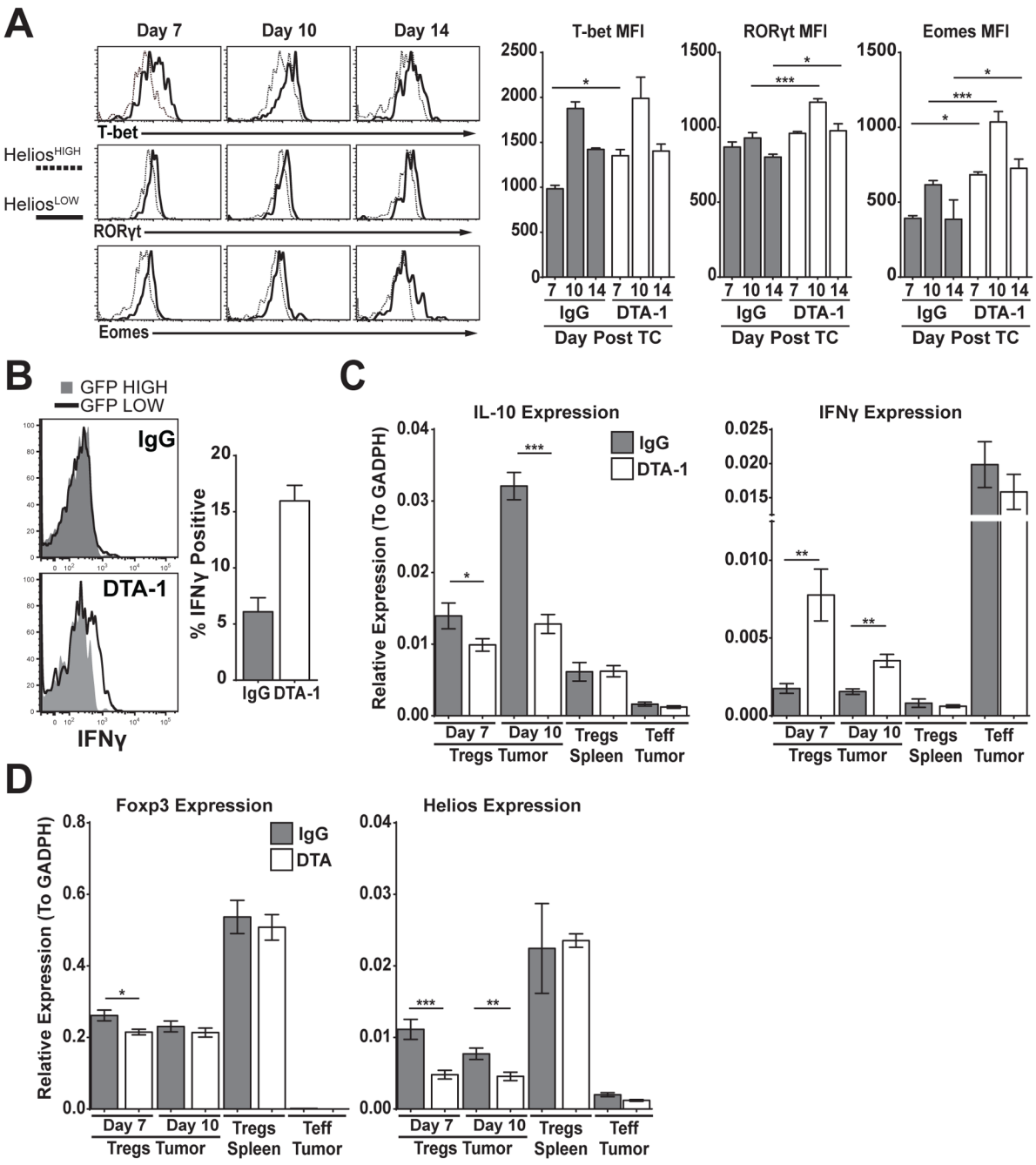

FIGURE 3. DTA-1-treated Treg display a Teff like profile

A) Helios expression compared to T-bet, RORγt and Eomes in Treg ($CD45^+$, $CD3^+$, $CD4^+$) from DTA-1-treated tumors is shown in representative plots. Graphs show the mean +/− SEM for MFI of these markers for IgG Treg, compared to DTA-1-modulated $Helios^{LOW}$ Treg at each timepoint. **B)** IFNγ recall expression in GFP high (gray shaded) compared to GFP low Treg (black line) from day 10 IgG- and DTA-1-treated tumors. Graph shows the mean +/− SEM IFNγ expression in IgG Treg, compared to GFP low DTA-1 Treg. **C&D)** Treg and Teff were sorted from individual mice as described in methods from indicated tissue and timepoints for gene expression analysis. Graphs compare the level of IL-10, IFNγ

(C), Foxp3 and Helios (D) expression in IgG- compared to DTA-1-treated tumors. Splenic Treg and tumor Teff are provided as controls. Experiments were repeated 3 times with N=4–5 (A,B) and 2 times with N=10 (C,D), with one representative experiment shown. * = $p<0.01$, **= $p<0.001$, ***=$p<0.0001$.

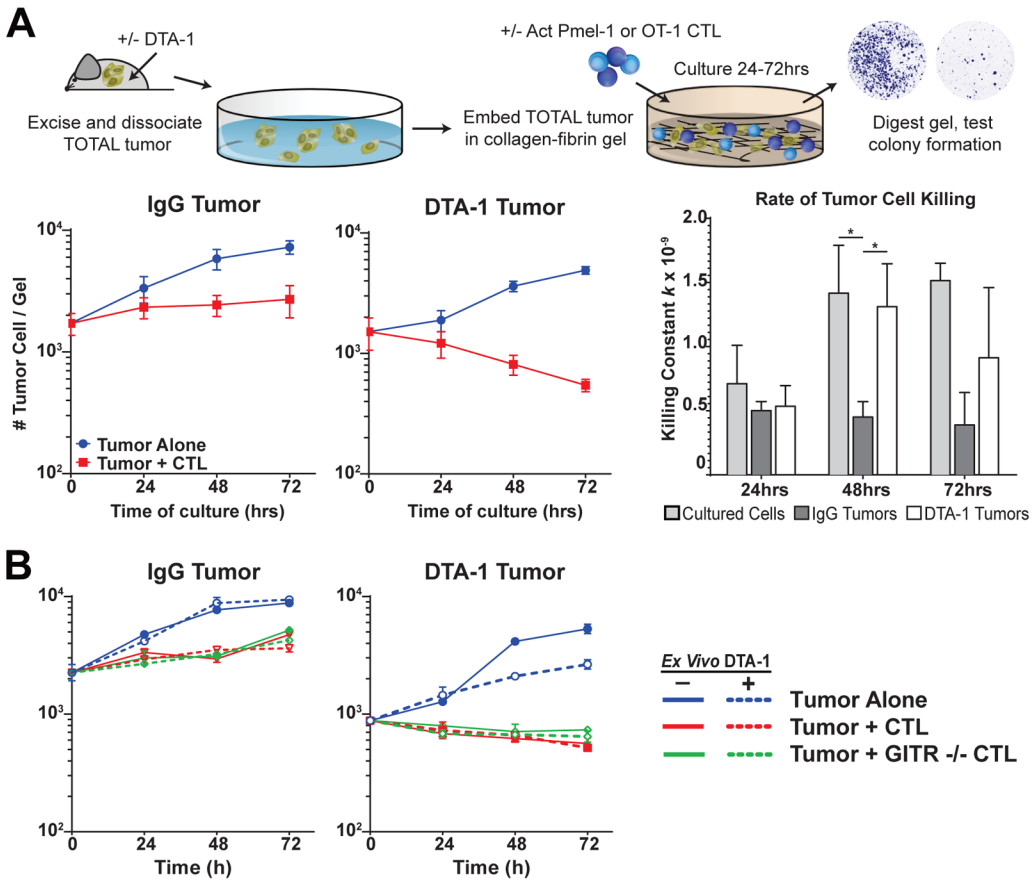

FIGURE 4. Treg lineage instability removes intra-tumor immune suppression

A,B) *Experiment schematic:* Tumors were isolated, dissociated and 10,000 live tumor cells were then embedded along with all tumor infiltrating cells (~3–5× tumor cell counts) in collagen-fibrin gel together with or without CTLs as described in methods. After 24, 48 and 72 hours, gels were lysed and viable cells were cultured in a colony-forming assay. No killing would appear with 100+ colonies, killing would show very few colonies. **A)** Graphs show number of viable tumor cells recovered at indicated timepoints for IgG (left) and DTA-1 (middle) for total tumors alone (blue line) or with activated OT-1 T cells (red line). (Right) Rate of B16 cell killing by OT-1 CTL (killing constant ***k***, as calculated in methods), of IgG (dark gray) and DTA-1 (white) tumors is shown compared to primary tissue culture B16 cells alone (light gray). **B)** Viable tumor cells recovered from cultures of IgG- and DTA-1-treated total tumors alone (blue), with $GITR^{+/+}$ Pmel-1 (red), and $GITR^{-/-}$ Pmel-1 (green). Dashed lines indicate cultures that included the *ex vivo* addition of 10μg/ml of DTA-1, solid ones indicate control cultures. Experiments were repeated 3 times with tumors pooled from 3–5 mice for each experiment. Mean and +/− SEM of 3 experiments is shown in A, a representative experiment is shown in B. * = $p<0.01$.